

Multi-Prompt with Depth Partitioned Cross-Modal Learning

Yiqi Wang

wangyiqi18@mails.ucas.ac.cn

School of Computer Science and Technology, University of
Chinese Academy of Sciences
Beijing, China

Zheng Zhu

zhengzhu@ieee.org

PhiGent Robotics
China

Guoxian Da

xianda_guo@163.com

PhiGent Robotics
China

Yingjie Tian*

tyj@ucas.ac.cn

Research Center on Fictitious Economy and Data Science,
University of Chinese Academy of Sciences
China

ABSTRACT

In recent years, soft prompt learning methods have been proposed to fine-tune large-scale vision-language pre-trained models for various downstream tasks. These methods typically combine learnable textual tokens with class tokens as input for models with frozen parameters. However, they often employ a single prompt to describe class contexts, failing to capture categories' diverse attributes adequately. This study introduces the Partitioned Multi-modal Prompt (PMPO), a multi-modal prompting technique that extends the soft prompt from a single learnable prompt to multiple prompts. Our method divides the visual encoder depths and connects learnable prompts to the separated visual depths, enabling different prompts to capture the hierarchical contextual depths of visual representations. Furthermore, to maximize the advantages of multi-prompt learning, we incorporate prior information from manually designed templates and learnable multi-prompts, thus improving the generalization capabilities of our approach. We evaluate the effectiveness of our approach on three challenging tasks: new class generalization, cross-dataset evaluation, and domain generalization. For instance, our method achieves a 79.28 harmonic mean, averaged over 11 diverse image recognition datasets (+7.62 compared to CoOp), demonstrating significant competitiveness compared to state-of-the-art prompting methods. The code is available [PMPO](#).

1 INTRODUCTION

In recent years, large-scale vision-language pre-trained models have shown significant potential for various downstream tasks and datasets [9, 42–44]. Utilizing contrastive learning, these models leverage large amounts of text-image pairs to train text and image encoders [31]. After pre-training, the text encoder transforms language prompts (e.g., "a photo of [class]") into text embeddings and calculates similarities with visual embeddings for image class prediction.

Despite the benefits of language-guided supervision in exploring open-set visual concepts, these models often exhibit sensitivity to manually designed template prompts for different datasets [31]. Recent studies have introduced various soft prompt learning methods [43, 44], which convert contextual prompt words into learnable vectors, demonstrating improved effectiveness and stability on downstream tasks compared to manually designed prompts.

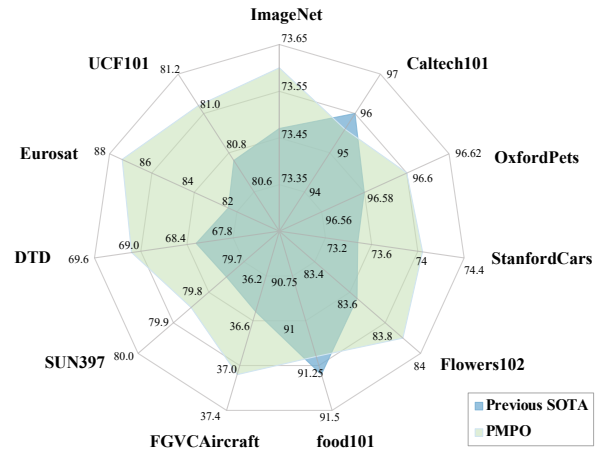


Figure 1: PMPO outperforms previous state-of-the-art models on 9 out of 11 diverse recognition datasets for the new classes generalization task.

This work addresses the limitations of existing soft prompt learning techniques. Traditional prefix prompt methods learn a single contextual template, yet describing diverse characteristics of each category may necessitate multiple descriptions. For example, combining two prefix templates, "[class] is a black and white striped animal" and "[class] looks like a horse," can effectively classify "zebra," "donkey," and "panda" better than using only one of them. So, we expand the single learnable prompts to multiple prompts for a more comprehensive representation of class context.

In Figure.2, we visualize the score-CAM [38] to elucidate the key motivation of PMPO. To learn discriminative multi-prompts, a naive approach entails matching visual embeddings with the corresponding category means of multi prompt embeddings. However, this method yields trivial solutions due to the absence of training differentiation for different prompts, merely aligning them with global visual embeddings. To overcome this issue, we introduce PMPO, a multi-modal prompts technique that partitions the visual encoder depth and connects learnable prompts to partitioned visual depths. This enables different prompts to learn the hierarchical contextual depths of visual representations.

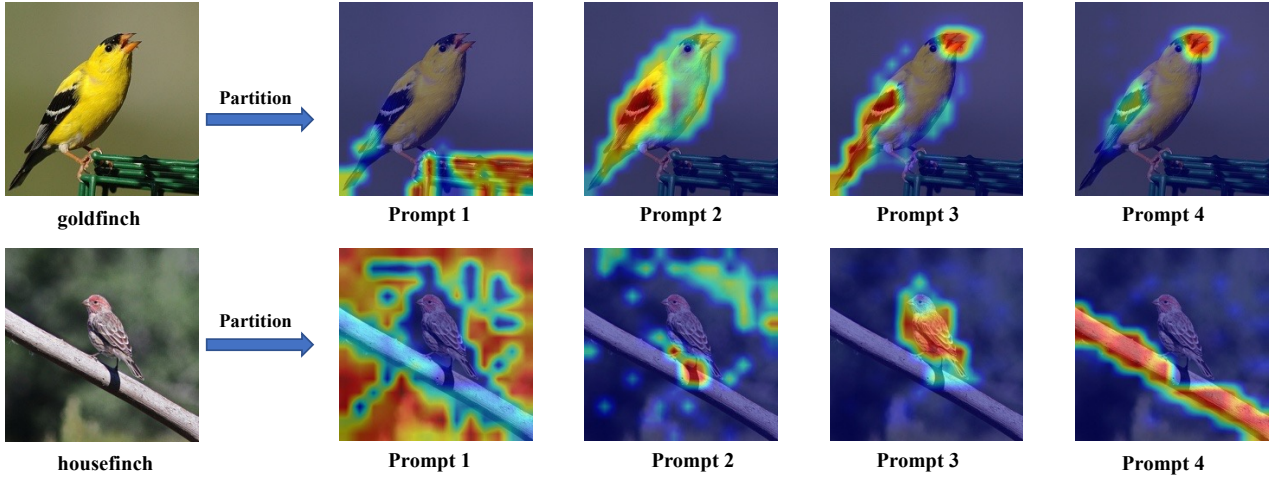


Figure 2: Key motivation of PMPO. We visualize the Score-CAM results for each prompt on two ImageNet samples. It is clear that different prompts indeed focus on distinct attributes of the classes. This observation highlights the importance of capturing diverse characteristics for effective recognition, as it allows the model to better understand various aspects of each class, leading to more accurate and robust predictions.

We evaluate our method on 11 datasets covering diverse visual recognition tasks, including base-to-new generalization, cross-dataset evaluation, and domain generalization settings. Experimental results in Figure.1 demonstrate that PMPO surpasses existing state-of-the-art prompt learning approaches, achieving absolute average gains in both base and new categories, as well as harmonic mean. Furthermore, PMPO exhibits superior generalization capability and robustness in transfer and domain generalization settings. In summary, the primary contributions of this work are:

- We propose depth-partitioned multi-modal prompts learning to leverage large-scale pre-trained vision-language models and capture the diverse characteristics of each category.
- To mitigate trivial solutions in multi-prompt learning, we introduce depth-partitioned multi-modal prompts, which serve as a bridge between learnable prompts and visual contextual features at different depths.
- We conduct extensive experiments on our proposed method, PMPO, showcasing exceptional performance across all few-shot recognition settings. These experiments highlight the comprehensive capabilities of PMPO.

2 RELATED WORK

Vision-Language Pre-trained Models: Vision-Language Pre-trained (VLP) models aim to establish cross-modal connections between visual and language modalities through comprehensive pre-training [4, 21, 22]. Various pre-training objectives have been introduced, which allow the categorization of VLP methods into different groups based on their goals, including (masked) language modeling [23, 39], image-text contrastive learning [14, 15, 31], image-text matching [1, 23], and combined approaches that merge the previously mentioned techniques [21, 22]. Most VLP approaches employ

pre-training using large-scale image-text pair datasets. For example, the CLIP model [31] leverages 400 million image-text pairs in its contrastive learning process. Consequently, VLP models have demonstrated significant advancements in few-shot visual recognition tasks [9, 31, 42–44], highlighting their capacity to improve open-world visual comprehension through language support.

Prompt Learning: Prompt learning was initially explored within Natural Language Processing (NLP) [30]. Recent studies have found that language model performance can be sensitive to input prompts [24, 27], leading to the development of methods to improve prompt learning using automatic prompt search [24, 33, 34] and prompt tuning [20].

Instead of manually creating prompts, Jiang et al. [17] use text mining and paraphrasing to generate a group of possible prompts, choosing the best ones based on their training accuracy. Shin et al. [35] present AutoPrompt, an approach that uses gradients to find the most influential tokens in a vocabulary. Concurrently, recent research in contrastive-learning-based Vision-Language Models (VLMs) [31] suggests learning virtual text as part of texts during the inference process.

Recently, CoOp [44], and its related version, CoCoOp [43], have integrated prompt learning into open-world visual understanding, enabling knowledge transfer from large-scale visual-language pre-trained models and significantly improving few-shot visual recognition performance. Maple [18] employs learning across multiple transformer blocks in both vision and language areas to understand the combined behavior of both modalities progressively. However, maple is a single-prompt method and couldn't give an insightful explanation of the design. KgCoOp [41] boosts the generalization capacity of learnable prompts for unseen classes, reducing the gap between learnable and hand-crafted prompts. The PLOT method

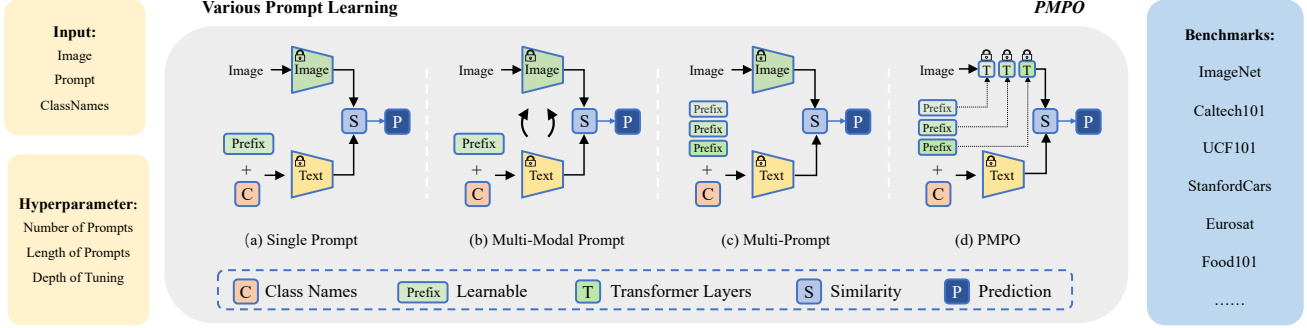


Figure 3: Graphical illustration of different prompt learning methods. The image encoder and text encoder are pre-trained on large-scale image-text pairs and remain frozen during prompt tuning. This figure provides a brief comparison of single-prompt, multi-prompt, multi-modal prompt, and our proposed PMPO method.

[3] is a multi-prompt learning method that enhances prompt learning by using optimal transport distance [26] to learn multiple local prompts, achieving more detailed vision-language matching. However, PLOT utilizes local features before the pooling operator, making it unsuitable for transformer-based methods. Additionally, it is a single-modal approach that lacks cross-modal connections, which are crucial for effectively integrating visual and language information. A comparison of these techniques with our method is shown in Figure.3.

3 METHODS

Figure 4 shows an overview of our method. PMPO first encodes multiple learnable language prompts using a pre-trained text encoder (with an optional manually-designed prompt). Then, PMPO extracts visual features using a partitioned visual encoder. By default, PMPO employs the ViT-B [7] as its visual encoder and partitions its transformer blocks. For each partitioned transformer block, PMPO utilizes the Deep Visual Prompt Tuning (D-VPT) [16] approach with visual context prompts projected from the corresponding learnable language prompt by linear layers. The final prediction is calculated using the mean of multi-prompt embeddings and visual embeddings. To better introduce the method, we first briefly review the CLIP (Contrastive Language-Image Pretraining) model [31], which has demonstrated remarkable performance in various tasks. We then introduce multi-prompt learning and partitioned multi-modal prompt learning to extend the applicability of CLIP-like models.

3.1 Preliminaries

Revisiting CLIP: CLIP consists of two primary components: an image encoder (either a ResNet [10], or a ViT [7]) and a text encoder (based on the Transformer architecture). The image encoder’s purpose is to transform input images into feature embeddings, while the text encoder generates vectorized representations for word token sequences. During training, CLIP utilizes a contrastive loss function to learn a joint embedding space between images and text.

Given a mini-batch containing image-text pairs, CLIP aims to maximize the cosine similarity between each image and its corresponding text while minimizing the cosine similarities between the

image and all other non-matching texts. This process is symmetrically applied to the text as well. Once trained, CLIP can be employed for zero-shot image recognition tasks. For the image encoder, let x represent the image features. For the text encoder, let $\{w_i\}_{i=1}^K$ denote a set of weight vectors produced, each representing a category. Specifically, each w_i originates from a prompt, such as "a photo of a {class}", where the i -th class name replaces the "{class}" token. The probability distribution over the class labels can be expressed as:

$$P(y|x) = \frac{\exp(\text{sim}(x, w_i)/\tau)}{\sum_{i=1}^K \exp(\text{sim}(x, w_i)/\tau)} \quad (1)$$

In this equation, $\text{sim}()$ indicates cosine similarity and τ refers to a learned temperature parameter.

Prompt Learning: To better adapt to downstream tasks, CoOp introduces a novel approach that replaces the previous "a photo of a" template with M learnable context vectors denoted as $p = [p_1, p_2, \dots, p_M]$, which have the same dimensions as word embeddings. For the i -th class, represented as c_i , the prompt changes to $t_i = \{p, c_i\}$. Here, c_i represents the word embedding(s) for the relevant class name, and p represents the shared context vectors across all classes. The text encoder, denoted as $T(\cdot)$, is used to predict the probability of an input image x belonging to a specific class y . The prediction probability is given by

$$P(y|x) = \frac{\exp(\text{sim}(x, T(t_i))/\tau)}{\sum_{i=1}^K \exp(\text{sim}(x, T(t_i))/\tau)} \quad (2)$$

To train CoOp for image recognition tasks, we employ a cross-entropy loss function and update context vectors during training. The base CLIP model remains frozen throughout the process.

3.2 PMPO

Multi-Prompt Learning: Though traditional soft prompt learning has shown impressive performance in classification tasks, it relies on a single prompt to characterize the context of classes. To effectively capitalize on the full extent of the CLIP pre-trained knowledge, we introduce a set of N text prompts, denoted as $P' = \{p^n | n = 1, \dots, N\}$. Each prompt, $P^n = [p_1^n, p_2^n, \dots, p_M^n]$, comprises

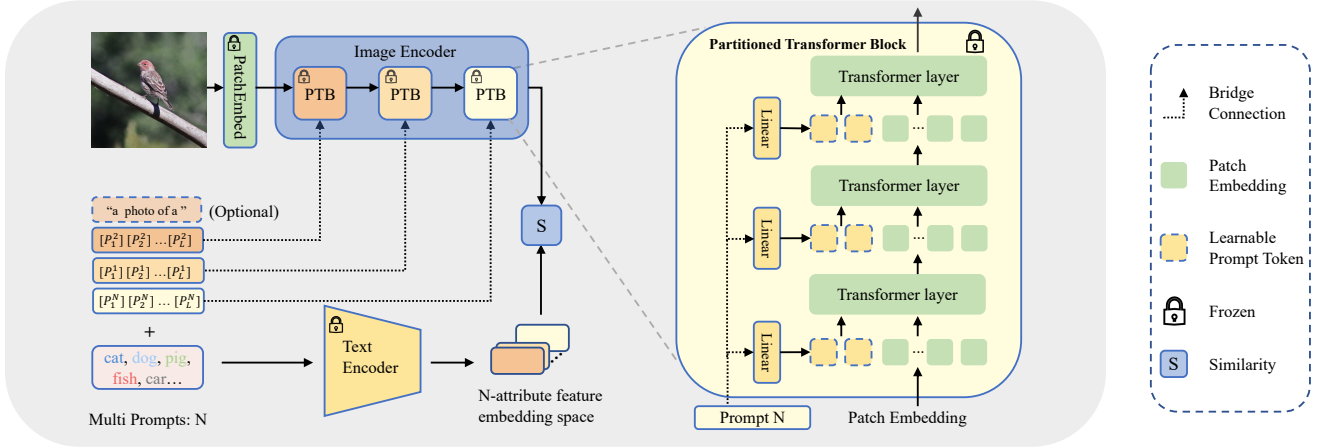


Figure 4: Overview of the PMPO training pipeline: PMPO is based on the frozen CLIP. N learnable prefix prompts establish bridge connections with Partitioned Transformer Blocks (PTB) enabling multi-prompts to learn hierarchical contextual visual representations. Within the PTB, Deep Visual Prompt Tuning is utilized for extracting visual embeddings. Furthermore, the ensemble of multi-prompts is computed within the feature embedding space, enhancing the overall effectiveness of the model.

exclusively trainable context tokens derived from the text encoder module, with M representing the length of these tokens.

The multi-prompts, denoted by $t' = \{t^n | n = 1, \dots, N\}$ and $t_i^n = \{p^n, c_i\}$, are generated by prepending the text prompts P' to the i -th tokenized class names. Notably, the text prompts P^n are consistently shared among all class names. Here, c_i corresponds to the word embedding associated with each class name.

We compute the mean of text features in the embedding space to process these multi-prompts. Subsequently, the prediction probability is denoted by the following equation:

$$P(y|x) = \frac{\exp(\text{sim}(x, T_i^*/\tau))}{\sum_{i=1}^K \exp(\text{sim}(x, T_i^*/\tau))} \quad (3)$$

$$T_i^* = \text{mean}(T(t_i^n))_{n=1 \dots N} \quad (4)$$

Utilizing multi-prompts offers advantages over the single-prompt approach, particularly in their ability to capture various aspects and attributes of a class. By employing multiple prompts, the model can describe different facets of a class, providing a more comprehensive representation. This leads to a deeper understanding of the class context and improved model performance. **Cross-Modal Depth-Partitioned Learning:** Directly using multi-prompts can lead to a trivial solution problem, as there is no explicit indication that the prompts are distinct for the model. To address this issue, we propose cross-modal depth-partitioned learning. We use a linear projection $f(\cdot)$ for each learnable prompt to map it to different levels of image encoder blocks. In the case of CLIP, we assign the N learnable prompts to various transformer blocks. We set the depth of the transformer to D , and each prompt is assigned to D/N blocks, ranging from shallow to deep layers. Following the visual-prompt tuning (VPT) [16] symbol definition, we compute a sequence of vectors $\{V_1, V_2, \dots, V_D\}$ using the function g with text

prompts $\{p^1, p^2, \dots, p^N\}$ as input:

$$V_1, V_2, \dots, V_D = g(p^1, \dots, p^N) \quad (5)$$

We then use these vectors to compute a series of embeddings $[x_i, E_i]$ using a set of layers L_i , where x_i is the embedding for the $[cls]$ token at layer L_{i+1} 's input space:

$$[x_i, E_i] = L_i([x_{i-1}, V_{i-1}, E_{i-1}]), \quad i = 1, 2, \dots, D \quad (6)$$

Here, $[\cdot, \cdot]$ indicates stacking and concatenation, and the resulting embedding $[x_i, V_i, E_i]$ has dimensions of $R^{(1+M+m) \times d}$. Each layer L_i in the network comprises Multiheaded Self-Attention (MSA), Feed-Forward Networks (FFN), LayerNorm, and residual connections. We map the final layer's $[CLS]$ embedding x to a predicted class probability distribution using Equation 3, which can be replaced by conditioned $x(p^1, p^2, \dots, p^N)$:

$$P(y|x) = \frac{\exp(\text{sim}(x(p^1, p^2 \dots p^N), T_i^*/\tau))}{\sum_{i=1}^K \exp(\text{sim}(x(p^1, p^2 \dots p^N), T_i^*/\tau))} \quad (7)$$

T_i^* is the mean of the encoded text embeddings. **Ensemble the Manual Prompt:** Another advantage of multi-prompt learning lies in the ability to utilize manually created prompts as prior information, which can be combined with multiple learnable prompts to generate the final text features. As detailed in CoCoOp [43], learnable prompt can improve classification performance for base classes, but may often result in overfitting. Conversely, the vanilla CLIP [31] typically demonstrates superior generalization capabilities when employing manual prompt. Thus, our framework can benefit from both manual and learnable prompts by employing the following formulation:

$$T_i^* = \text{mean}([T(t_i^1), T(t_i^2), \dots, T(t_i^N), T(t_i^{\text{prior}})]) \quad (8)$$

Table 1: Comparison of our approach with state-of-the-art methods in the base-to-new generalization setting,utilizing $N = 4$ learnable prompts with a manual prompt. All results are trained on 16-shot samples from the base classes, with the ViT-B/16 backbone architecture. H:Harimonic mean

(a) Average over 11 datasets				(b) ImageNet				(c) Caltech101			
	Base	New	H		Base	New	H		Base	New	H
CLIP	69.34	74.22	71.70	CLIP	72.43	68.14	70.22	CLIP	96.84	94.00	95.40
CoOp	82.69	63.22	71.66	CoOp	76.47	67.88	71.92	CoOp	98.00	89.81	93.73
CoCoOp	80.47	71.69	75.83	CoCoOp	75.98	70.43	73.10	CoCoOp	97.96	93.81	95.84
MaPLe	82.27	75.14	78.55	MaPLe	76.66	70.54	73.47	MaPLe	97.74	94.36	96.02
KgCoOp	80.73	73.60	77.00	KgCoOp	75.83	69.96	72.78	KgCoOp	97.72	94.39	96.03
PMPO	82.91	75.95	79.27	PMPO	76.94	70.55	73.60	PMPO	98.04	93.34	95.63
(d) OxfordPets				(e) StanfordCars				(f) Flowers102			
	Base	New	H		Base	New	H		Base	New	H
CLIP	91.17	97.26	94.12	CLIP	63.37	74.89	68.65	CLIP	72.08	77.80	74.83
CoOp	94.24	96.66	95.43	CoOp	78.12	60.40	68.13	CoOp	97.60	59.67	74.06
CoCoOp	95.20	97.69	96.43	CoCoOp	70.49	73.59	72.01	CoCoOp	94.87	71.75	81.71
MaPLe	95.43	97.76	96.58	MaPLe	72.94	74.00	73.47	MaPLe	95.92	72.46	82.56
KgCoOp	94.65	97.76	96.18	KgCoOp	71.76	75.04	73.36	KgCoOp	95.00	74.73	83.65
PMPO	95.84	97.37	96.60	PMPO	74.16	74.15	74.16	PMPO	97.12	73.85	83.89
(g) Food101				(h) FGVC Aircraft				(i) SUN397			
	Base	New	H		Base	New	H		Base	New	H
CLIP	90.10	91.22	90.67	CLIP	27.19	36.29	31.09	CLIP	69.36	75.35	72.23
CoOp	88.33	82.26	85.19	CoOp	40.44	22.30	28.75	CoOp	80.60	65.89	72.51
CoCoOp	90.70	91.29	90.99	CoCoOp	33.41	23.71	27.74	CoCoOp	79.74	76.86	78.27
MaPLe	90.71	92.05	91.38	MaPLe	37.44	35.61	36.50	MaPLe	80.82	78.70	79.75
KgCoOp	90.05	91.70	91.09	KgCoOp	36.21	33.55	34.83	KgCoOp	80.29	76.53	78.36
PMPO	90.58	91.86	91.22	PMPO	38.46	35.99	37.18	PMPO	81.54	78.22	79.85
(j) DTD				(k) Eurosat				(l) UCF101			
	Base	New	H		Base	New	H		Base	New	H
CLIP	53.24	59.90	56.37	CLIP	56.48	64.05	60.03	CLIP	7530	77.50	73.85
CoOp	79.44	41.18	54.24	CoOp	92.19	54.74	68.69	CoOp	84.69	56.05	67.46
CoCoOp	77.01	56.00	64.16	CoCoOp	87.49	60.04	71.21	CoCoOp	82.33	73.45	77.64
MaPLe	80.36	59.18	68.16	MaPLe	94.07	73.23	82.35	MaPLe	83.00	78.66	80.77
KgCoOp	77.55	54.99	64.35	KgCoOp	85.64	64.34	73.48	KgCoOp	82.89	76.67	79.65
PMPO	80.21	60.95	69.27	PMPO	94.24	81.85	87.41	PMPO	84.85	77.64	81.09

4 EXPERIMENT

Following the previous work, CoOp [44], and CoCoOp [43], we primarily evaluate our method in the following settings: 1) generalization from base to new classes within a dataset; 2) cross-dataset transfer; 3) domain generalization. All models used in our experiments are based on the open-source CLIP [31]. We also conducted an ablation study on the hyperparameters and discussed their effects. Before delving into the results, we provide the details of the experimental setup below.

Datasets: In our study, we focus on two primary settings: base-to-new generalization and cross-dataset transfer. We utilize 11 image recognition datasets from Zhou et al.[44], encompassing a wide array of recognition tasks. The benchmark includes ImageNet [6] and Caltech101 [8] for generic object classification; OxfordPets [29], StanfordCars [19], Flowers102 [28], Food101 [2], and FGVC Aircraft [25] for fine-grained classification; SUN397[40] for scene recognition; UCF101 [36] for action recognition; DTD [5] for texture classification; and EuroSAT [11] for satellite imagery recognition.

For domain generalization experiments, we employ ImageNet as the source dataset and four ImageNet variants with distinct domain shifts as target datasets: ImageNetV2 [32], ImageNet-Sketch [37],

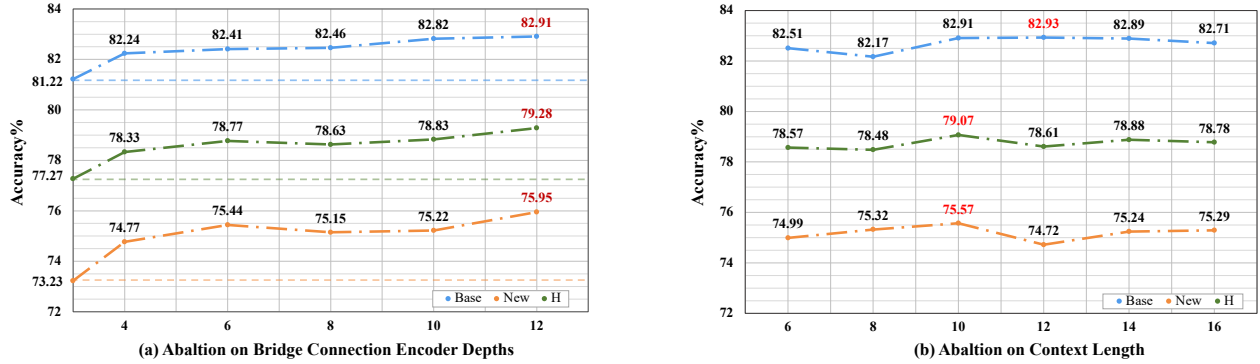


Figure 5: Ablation the bridge connection depths and contextual length, The results are the average of 11 datasets’ accuracy

ImageNet-A [13], and ImageNet-R [12]. In line with CoOp, we randomly sample a 16-shot training set for each dataset and use the original test set for evaluation. Results are averaged across three runs with different seeds.

Training Details: In our experiments, we employ ViT-B/16 [44] as the backbone of CLIP. We adopt a few-shot training strategy with 16 shots randomly sampled using different seeds. For the base-to-new generalization experiment, we set the number of prompts to 4 by default, the bridge depth to 12 (considering both vision transformer layers), and the contextual token length to 10. Regarding other hyperparameters, we follow CoOp’s configuration, using the SGD optimizer with an initial learning rate of 0.002 and a batch size of 8 with 6 epochs for most datasets, except for ImageNet, which maintains a learning rate of 0.01 and a batch size of 32. The learning rate is decayed using cosine annealing, and the optimizer warms up with a 1e-5 learning rate. For domain transfer and cross-dataset experiments, we adopt CoCoOp’s settings, which suggest that shorter context lengths yield better performance and stronger robustness to domain shift. Thus, we set the token length to 4, and the learning rate is set to 0.01 with 2 epochs. The other parameters remain the same as in the base-to-new experiments. All experiments are conducted on 4 Nvidia RTX3090 GPUs. For a fair comparison, all the results are averaged over three different seeds.

4.1 Generalization From Base-to-New Classes

We build upon the work of CoOp[44] and divide each of the 11 recognition datasets into two parts: base classes and new classes. We train PMPO on the base classes and evaluate its performance on the new classes, comparing our method with five baselines: CLIP[31], CoOp[44], CoCoOp[43], Maple[18], and KgCoOp[41]. Here, we provide a brief overview of these five baseline methods: CLIP[31] utilizes a manually-designed template, typically employing "a photo of [cls]" as the text encoder prompt. CoOp[44] replaces the manually-designed prompt with a single learnable prompt. CoCoOp[43] incorporates a conditioned single learnable prompt. Maple[18] represents a state-of-the-art approach using multi-modal language-vision prompts. KgCoOp[41] leverages prior information from fixed, manually-designed CLIP prompts to train learnable prompts via knowledge distillation. The results of our method and the baselines are presented in Table 1.

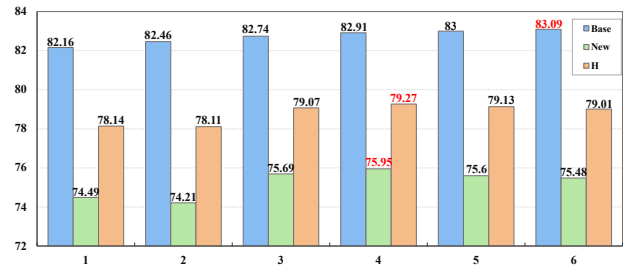


Figure 6: Ablation number of prompts

Significant Improvement in Base Classes: As shown in Table 1, our proposed PMPO achieves the best performance on base classes for 6 out of 11 datasets, as well as the best average performance across base classes when compared to the baseline methods. Generally, higher performance on base classes can result in overfitting and reduced generalizability to new classes. Among existing state-of-the-art methods, CoOp is the previous best method on the base classes, but it typically exhibits an overfitting problem, as argued by CoCoOp. However, PMPO significantly outperforms CoOp on the average of 11 datasets (82.69% vs. 82.91%) while improving generalization ability on new classes. This exceptional performance demonstrates PMPO’s robust capability to adapt to downstream tasks based on pre-trained CLIP. In the ablation study (Section 4.2), we will discuss the relationship between increasing the number of prompts and improving base classes’ accuracy. **Generalization to New Classes:** With improvements in base classes, PMPO also enhances generalization on new classes for the average unseen accuracy across all 11 datasets. Specifically, CLIP, KgCoOp, Maple, and PMPO achieve the best-unseen accuracy on the 2/11, 3/11, 3/11, and 3/11 datasets, respectively. While CoOp overfits base classes, CoCoOp improves generalization ability through image conditional context learning, while KgCoOp enhances it using knowledge-guided context optimization. However, they all underperform compared to CLIP in new classes. In contrast, PMPO surpasses CLIP on 7/11 datasets and demonstrates a 1.73% improvement on average across datasets for new classes. PMPO also performs better generalization than the previous best method, Maple (75.12% vs. 75.95%) for new class generalization. It is worth mentioning that PMPO significantly outperforms Maple on Eurosat [11], with an impressive 8.52% improvement. When considering

Table 2: Comparison of PMPO with other methods in domain generalization setting.

	Source		Target		
	Imagnet	ImageNetV2	ImageNet-Sketch	ImageNet-A	ImageNet-R
CLIP	66.73	60.83	46.15	47.77	73.96
CoOp	71.51	64.20	47.99	49.71	75.21
CoCoOp	71.02	64.07	48.75	50.63	76.18
MaPLe	70.72	64.07	49.15	50.90	76.98
KgCoOp	71.20	64.20	48.97	50.69	76.70
PMPO	70.78	64.20	49.64	50.63	77.12

base and new classes, PMPO achieves the best harmonic mean on 9 out of 11 datasets and attains the highest average performance, underlining its effectiveness and robustness in adapting to diverse tasks.

4.2 Abalitation Study

Number of Prompts: To analyze the impact of the number of prompts, we conducted experiments on 11 datasets. We compared the average base, new, and harmonic mean accuracy performance, as shown in Figure 6. All experiments were conducted with depth $D = 12$ and length $L = 10$ while varying the number of prompts from $N = 1$ to $N = 6$. Further analysis of the results reveals a continuous improvement in base accuracy performance as the number of prompts increases (from 82.16% to 83.09%), which demonstrates the enhanced fitting ability of the multi-prompt strategy. However, for new classes, generalization performance increases when the number of prompts ranges from $N = 1$ to $N = 4$. When $N > 4$, PMPO begins to overfit on base classes, leading to a decline in the performance of unseen classes. Considering both base and new classes, $N = 4$ is clearly the optimal setting.

Table 3: Effect of ensembling the manually-designed prompt on the base-to-new generalization on 11 datasets. M means the manually-designed prompt. H :Harmonic mean.

datasets	Base		New		H	
	w/o M	w/i M	w/o M	w/i M	w/o M	w/i M
Imagnet	77.11	76.94	70.45	70.55	73.62	73.60
Caltech101	98.34	98.04	93.27	93.24	95.74	95.63
OxfordPets	95.78	95.84	97.45	97.37	96.61	96.60
StanfordCars	74.76	74.16	74.06	74.15	74.41	74.16
Flowers102	96.68	97.12	71.87	73.85	83.36	83.89
Food101	90.52	90.58	91.50	91.80	91.00	91.22
FGVCAircraft	38.14	38.46	34.95	35.99	36.47	37.18
SUN397	81.54	81.71	77.80	78.22	79.71	79.85
DTD	81.33	80.21	59.54	60.95	68.75	69.27
EuroSAT	93.73	94.24	78.14	81.85	85.23	87.41
UCF101	85.06	84.85	76.74	77.64	80.69	81.09
Average	83.01	75.09	82.91	75.95	78.85	79.27

Table 4: Ablation on alternative prompt learning design. SS:Single-Prompt with Sing-Modal, MS: Multi-Prompt with Sing-Modal, SM: Single-Prompt with Multi-Modal, H: Harmonic mean.

Method	Base	New	H
CoOp-SS	82.69	63.22	71.66
PMPO-MS	81.22	73.23	77.27
PMPO-SM	82.16	74.49	78.14
PMPO	82.91	75.95	79.27

Bridge Connection Depths and Context Length: In Figure.5, we examine the impact of varying depths, which bridge the text encoder prompts and visual encoder blocks. For this ablation study, the number of prompts (N) is set to 4. We obtain a single-modal multi-prompt model when the depth is set to 0. This vanilla model directly matches the multi-prompt ensemble with the visual features, resulting in the lowest average performance across 11 datasets, with base accuracy at 73.23%, new accuracy at 73.23%, and harmonic mean (H) at 81.22%. In contrast, the default setting with depths set to 12 outperforms the vanilla setting by 2.72% on base, 2.01% on new, and 1.69% on H . This improvement might be attributed to the vanilla model’s tendency to learn trivial solutions without comprehensive prompts. This comparison demonstrates that our partitioned cross-modal design significantly enhances the performance of multi-prompt learning.

Ensembling Manually-Designed Prompt: As shown in Figure.3, we evaluate PMPO in two different settings across 11 datasets: without ensembling the manually-designed prompt and with it (default). In terms of results, the setting without a manually-designed prompt achieves better average accuracy on base classes. However, the setting with manually-designed prompts demonstrates stronger generalization performance on new classes (better on 10 out of 11 datasets than the setting without manual prompts). Therefore, we choose the setting with a manually-designed prompt as our default configuration.

Number of Shots: We investigate the performance of various K-shot samples across an average of 11 datasets for base-to-new settings, as shown in Figure.6. We sample K-shots by 4, 8, and 16 (default). As the number of shots increases, PMPO consistently performs better, with the harmonic mean rising from (75.59% to

Table 5: Comparison of PMPO in the cross-dataset transfer setting with other state-of-the-art methods. Prompts are trained on ImageNet with 16-shot per classes and applied to the 10 target datasets. Clearly, CoCoOp demonstrates better transferability than other methods.

	Source					Target						
	Imagnet	Caltech101	OxfordPets	StanfordCars	Flowers102	Food101	Aircraft	SUN397	DTD	EuroSAT	UCF101	Average
CoOp	71.51	93.70	89.14	64.51	68.71	85.30	18.47	64.15	41.92	46.39	66.55	63.88
CoCoOp	71.02	94.43	90.14	65.32	71.88	86.06	22.94	67.36	45.73	45.37	68.21	65.74
MaPLe	70.72	93.53	90.49	65.57	72.23	86.20	24.74	67.01	46.49	48.06	68.69	66.30
KgCoOp	70.66	93.92	89.83	65.41	70.01	86.36	22.51	66.16	46.35	46.04	68.60	65.51
PMPO	70.78	93.67	90.09	65.64	72.82	86.55	25.10	67.54	46.38	49.28	68.46	66.94

Table 6: Effect of number of shots on the base-to-new generalization on 11 datasets. *M* means the manually-designed prompt. H: Harmonic mean.

datasets	Base			New			H		
	4-shot	8-shot	16-shot	4-shot	8-shot	16-shot	4-shot	8-shot	16-shot
CoOp	78.43	80.73	82.69	68.03	68.39	63.22	72.44	73.50	71.66
CoCoOp	76.72	78.56	80.47	73.34	72.00	71.69	74.85	74.90	75.83
MaPLe	76.71	79.12	82.27	72.86	74.74	75.14	74.70	76.93	78.55
KgCoOp	79.92	78.36	80.73	73.11	73.89	73.60	75.90	76.60	77.00
PMPO	78.34	80.25	82.91	73.05	74.11	75.95	75.59	77.06	79.27

79.27%). PMPO achieves the best results on 8-shot and 16-shot settings, with superior scores of 76.93% vs. 77.06% and 78.55% vs. 79.27%, respectively. For the 16-shot setting, PMPO attains state-of-the-art performance for both base and new classes, as well as the harmonic mean. However, PMPO’s performance is slightly lower in the 4-shot setting (75.59% vs. 75.90%). This can be attributed to PMPO’s requirement to learn more prompts, and the limited low-shot samples are insufficient for learning discriminative prompts effectively.

Comparison with Alternative Designs: In Table 4, we present a simple comparison of other prompting designs. Since CoOp is defined as the single-prompt, single-modal method, we introduce two alternative methods: PMPO-MS, which uses multi-prompts (including manually-designed prompts) to replace the single learnable prompt and lacks a bridge connection between the text and image encoders; and PMPO-SM, which features a single-prompt with visual depth connections (one learnable prompt has connections with 12 visual transformer blocks). The results show that both PMPO-MS and PMPO-SM underperform compared to the multi-prompt, partitioned cross-modal PMPO approach.

4.3 Cross-dataset Transfer Evaluation

In Table 5, we assess the cross-dataset transfer generalization capability of PMPO by training the model on the entire 1000 classes of ImageNet[6] and testing its performance on 10 other diverse

datasets. The results indicate that PMPO outperforms other methods in 6 out of the 10 cross-dataset evaluation settings, with the highest average performance across all 11 datasets. The range of superior performance varies, from a 0.18% improvement (SUN397 compared with CoCoOp) to a 0.59% enhancement (Flowers102 compared with MaPLe). These findings underscore the competitive generalization ability of the PMPO approach, highlighting its adaptability across various datasets and settings.

4.4 Domain Generalization:

Domain Generalization aims to assess generalization by evaluating the trained model on a target dataset. Given CLIP’s robust performance in domain generalization, we also evaluate PMPO’s domain generalization ability by performing prompt tuning on few-shot ImageNet and testing PMPO on ImageNetV2, ImageNet-Sketch, ImageNet-A, and ImageNet-R. These datasets share the same classes but have different data distributions than the ImageNet domain. As shown in Table 2, although CoOp achieves the highest performance on the source ImageNet, its generalizability to a broader domain is weaker than CoCoOp. MaPLe and KgCoOp are also competitive methods, with MaPLe achieving the previous best performance in 3 out of 4 domain generalization settings. However, PMPO outperforms these methods on 3 target datasets. This comparison confirms that the partitioned multi-modal prompts in PMPO exhibit better domain generalization capabilities.

5 LIMITATIONS

Although PMPO demonstrates competitive performance, it should be noted that partitioned multi-prompt learning has two limitations: 1) PMPO demands more GPU memory than single-prompt learning. That is because the PMPO needs a multi-forward pass to the text encoder. Significantly as the number of prompts increases. This results in a linear growth of computational cost for the text encoder with respect to the number of classes. Future research may need to explore class sampling strategies to mitigate this issue. 2) The PMPO needs to be more shot for train than the other prompt tuning methods, as the table.6. Some data argument methods may help this.

6 CONCLUSION

In this paper, we introduce the Partitioned Multi-modal Prompt (PMPO), a novel approach that addresses the limitations of single-prompt learning in large-scale vision-language pre-trained models. By partitioning the visual encoder depths and connecting learnable prompts with the divided visual depths, our method enables different prompts to capture the hierarchical contextual depths of visual representations.

Through extensive experiments on 11 diverse image recognition datasets, we demonstrate that our proposed method, PMPO, achieves outstanding performance across new class generalization, cross-dataset evaluation, and domain generalization.

REFERENCES

- [1] Hangbo Bao, Wenhui Wang, Li Dong, Qiang Liu, Owais Khan Mohammed, Kriti Aggarwal, Subhojit Som, Songhao Piao, and Furu Wei. Vlm: Unified vision-language pre-training with mixture-of-modality-experts. *Advances in Neural Information Processing Systems*, 35:32897–32912, 2022.
- [2] Lukas Bossard, Matthieu Guillaumin, and Luc Van Gool. Food-101—mining discriminative components with random forests. In *Computer Vision—ECCV 2014: 13th European Conference, Zurich, Switzerland, September 6–12, 2014, Proceedings, Part VI* 13, pages 446–461. Springer, 2014.
- [3] Guangyi Chen, Weiran Yao, Xiangchen Song, Xinyue Li, Yongming Rao, and Kun Zhang. Plot: Prompt learning with optimal transport for vision-language models. In *The Eleventh International Conference on Learning Representations*.
- [4] Xi Chen, Xiao Wang, Soravit Changpinyo, AJ Piergiovanni, Piotr Padlewski, Daniel Salz, Sebastian Goodman, Adam Grycner, Basil Mustafa, Lucas Beyer, Alexander Kolesnikov, Joan Puigcerver, Nan Ding, Keran Rong, Hassan Akbari, Gaurav Mishra, Linting Xue, Ashish Thapliyal, James Bradbury, Weicheng Kuo, Mojtaba Seyedhosseini, Chao Jia, Burcu Karagol Ayan, Carlos Riquelme, Andreas Steiner, Anelia Angelova, Xiaohua Zhai, Neil Houlsby, and Radu Soricut. Pali: A jointly-scaled multilingual language-image model, 2022.
- [5] Mircea Cimpoi, Subhansu Maji, Iasonas Kokkinos, Sammy Mohamed, and Andreea Vedaldi. Describing textures in the wild. In *Proceedings of the IEEE conference on computer vision and pattern recognition*, pages 3606–3613, 2014.
- [6] Jia Deng, Wei Dong, Richard Socher, Li-Jia Li, Kai Li, and Li Fei-Fei. Imagenet: A large-scale hierarchical image database. In *2009 IEEE conference on computer vision and pattern recognition*, pages 248–255. Ieee, 2009.
- [7] Alexey Dosovitskiy, Lucas Beyer, Alexander Kolesnikov, Dirk Weissenborn, Xi-aohua Zhai, Thomas Unterthiner, Mostafa Dehghani, Matthias Minderer, Georg Heigold, Sylvain Gelly, et al. An image is worth 16x16 words: Transformers for image recognition at scale. *arXiv preprint arXiv:2010.11929*, 2020.
- [8] Li Fei-Fei, Rob Fergus, and Pietro Perona. Learning generative visual models from few training examples: An incremental bayesian approach tested on 101 object categories. In *2004 conference on computer vision and pattern recognition workshop*, pages 178–178. IEEE, 2004.
- [9] Peng Gao, Shijie Geng, Renrui Zhang, Teli Ma, Rongyao Fang, Yongfeng Zhang, Hongsheng Li, and Yu Qiao. Clip-adapter: Better vision-language models with feature adapters. *arXiv preprint arXiv:2110.04544*, 2021.
- [10] Kaiming He, Xiangyu Zhang, Shaoqing Ren, and Jian Sun. Deep residual learning for image recognition. In *Proceedings of the IEEE conference on computer vision and pattern recognition*, pages 770–778, 2016.
- [11] Patrick Helber, Benjamin Bischke, Andreas Dengel, and Damian Borth. Eurosat: A novel dataset and deep learning benchmark for land use and land cover classification. *IEEE Journal of Selected Topics in Applied Earth Observations and Remote Sensing*, 12(7):2217–2226, 2019.
- [12] Dan Hendrycks, Steven Basart, Norman Mu, Saurav Kadavath, Frank Wang, Evan Dorundo, Rahul Desai, Tyler Zhu, Samyak Parajuli, Mike Guo, et al. The many faces of robustness: A critical analysis of out-of-distribution generalization. In *Proceedings of the IEEE/CVF International Conference on Computer Vision*, pages 8340–8349, 2021.
- [13] Dan Hendrycks, Kevin Zhao, Steven Basart, Jacob Steinhardt, and Dawn Song. Natural adversarial examples. In *Proceedings of the IEEE/CVF Conference on Computer Vision and Pattern Recognition*, pages 15262–15271, 2021.
- [14] Aashi Jain, Mandy Guo, Krishna Srinivasan, Ting Chen, Sneha Kudugunta, Chao Jia, Yinfei Yang, and Jason Baldridge. Mural: multimodal, multitask retrieval across languages. *arXiv preprint arXiv:2109.05125*, 2021.
- [15] Chao Jia, Yinfei Yang, Ye Xia, Yi-Ting Chen, Zarana Parekh, Hieu Pham, Quoc Le, Yun-Hsuan Sung, Zhen Li, and Tom Duerig. Scaling up visual and vision-language representation learning with noisy text supervision. In *International Conference on Machine Learning*, pages 4904–4916. PMLR, 2021.
- [16] Menglin Jia, Luming Tang, Bor-Chun Chen, Claire Cardie, Serge Belongie, Bharath Hariharan, and Ser-Nam Lim. Visual prompt tuning. In *Computer Vision—ECCV 2022: 17th European Conference, Tel Aviv, Israel, October 23–27, 2022, Proceedings, Part XXXIII*, pages 709–727. Springer, 2022.
- [17] Zhengbao Jiang, Frank F Xu, Jun Araki, and Graham Neubig. How can we know what language models know? *Transactions of the Association for Computational Linguistics*, 8:423–438, 2020.
- [18] Muhammad Uzair Khattak, Hanoona Rasheed, Muhammad Maaz, Salman Khan, and Fahad Shahbaz Khan. Maple: Multi-modal prompt learning. *arXiv preprint arXiv:2210.03117*, 2022.
- [19] Jonathan Krause, Michael Stark, Jia Deng, and Li Fei-Fei. 3d object representations for fine-grained categorization. In *Proceedings of the IEEE international conference on computer vision workshops*, pages 554–561, 2013.
- [20] Brian Lester, Rami Al-Rfou, and Noah Constant. The power of scale for parameter-efficient prompt tuning. In *Proceedings of the 2021 Conference on Empirical Methods in Natural Language Processing*, pages 3045–3059, Online and Punta Cana, Dominican Republic, Nov. 2021. Association for Computational Linguistics.
- [21] Junnan Li, Dongxu Li, Silvio Savarese, and Steven Hoi. Blip-2: Bootstrapping language-image pre-training with frozen image encoders and large language models, 2023.
- [22] J. Li, D. Li, C. Xiong, and S. Hoi. Blip: Bootstrapping language-image pre-training for unified vision-language understanding and generation. 2022.

- [23] Junnan Li, Ramprasaath Selvaraju, Akhilesh Gotmare, Shafiq Joty, Caiming Xiong, and Steven Chu Hong Hoi. Align before fuse: Vision and language representation learning with momentum distillation. *Advances in neural information processing systems*, 34:9694–9705, 2021.
- [24] Yao Lu, Max Bartolo, Alastair Moore, Sebastian Riedel, and Pontus Stenetorp. Fantastically ordered prompts and where to find them: Overcoming few-shot prompt order sensitivity, 2022.
- [25] Subhransu Maji, Esa Rahtu, Juho Kannala, Matthew Blaschko, and Andrea Vedaldi. Fine-grained visual classification of aircraft. *arXiv preprint arXiv:1306.5151*, 2013.
- [26] Gaspard Monge. Mémoire sur la théorie des déblais et des remblais. *Mem. Math. Phys. Acad. Royale Sci.*, pages 666–704, 1781.
- [27] Feng Nie, Meixi Chen, Zhirui Zhang, and Xu Cheng. Improving few-shot performance of language models via nearest neighbor calibration. *arXiv preprint arXiv:2212.02216*, 2022.
- [28] Maria-Elena Nilsback and Andrew Zisserman. Automated flower classification over a large number of classes. In *2008 Sixth Indian Conference on Computer Vision, Graphics & Image Processing*, pages 722–729. IEEE, 2008.
- [29] Omkar M Parkhi, Andrea Vedaldi, Andrew Zisserman, and CV Jawahar. Cats and dogs. In *2012 IEEE conference on computer vision and pattern recognition*, pages 3498–3505. IEEE, 2012.
- [30] Fabio Petroni, Tim Rocktäschel, Patrick Lewis, Anton Bakhtin, Yuxiang Wu, Alexander H Miller, and Sebastian Riedel. Language models as knowledge bases? *arXiv preprint arXiv:1909.01066*, 2019.
- [31] Alec Radford, Jong Wook Kim, Chris Hallacy, Aditya Ramesh, Gabriel Goh, Sandhini Agarwal, Girish Sastry, Amanda Askell, Pamela Mishkin, Jack Clark, et al. Learning transferable visual models from natural language supervision. In *International conference on machine learning*, pages 8748–8763. PMLR, 2021.
- [32] Benjamin Recht, Rebecca Roelofs, Ludwig Schmidt, and Vaishaal Shankar. Do imagenet classifiers generalize to imagenet? In *International conference on machine learning*, pages 5389–5400. PMLR, 2019.
- [33] Ohad Rubin, Jonathan Herzig, and Jonathan Berant. Learning to retrieve prompts for in-context learning, 2022.
- [34] Taylor Shin, Yasaman Razeghi, Robert L. Logan IV, Eric Wallace, and Sameer Singh. AutoPrompt: Eliciting Knowledge from Language Models with Automatically Generated Prompts. In *Proceedings of the 2020 Conference on Empirical Methods in Natural Language Processing (EMNLP)*, pages 4222–4235, Online, Nov. 2020. Association for Computational Linguistics.
- [35] Taylor Shin, Yasaman Razeghi, Robert L Logan IV, Eric Wallace, and Sameer Singh. Autoprompt: Eliciting knowledge from language models with automatically generated prompts. *arXiv preprint arXiv:2010.15980*, 2020.
- [36] Khurram Soomro, Amir Roshan Zamir, and Mubarak Shah. Ucf101: A dataset of 101 human actions classes from videos in the wild. *arXiv preprint arXiv:1212.0402*, 2012.
- [37] Haohan Wang, Songwei Ge, Zachary Lipton, and Eric P Xing. Learning robust global representations by penalizing local predictive power. *Advances in Neural Information Processing Systems*, 32, 2019.
- [38] Haofan Wang, Zifan Wang, Mengnan Du, Fan Yang, Zijian Zhang, Sirui Ding, Piotr Mardziel, and Xia Hu. Score-cam: Score-weighted visual explanations for convolutional neural networks. In *Proceedings of the IEEE/CVF conference on computer vision and pattern recognition workshops*, pages 24–25, 2020.
- [39] Wenhui Wang, Hangbo Bao, Li Dong, Johan Bjorck, Zhiliang Peng, Qiang Liu, Kriti Aggarwal, Owais Khan Mohammed, Saksham Singhal, Subhojit Som, et al. Image as a foreign language: Beit pretraining for all vision and vision-language tasks. *arXiv preprint arXiv:2208.10442*, 2022.
- [40] Jianxiong Xiao, James Hays, Krista A Ehinger, Aude Oliva, and Antonio Torralba. Sun database: Large-scale scene recognition from abbey to zoo. In *2010 IEEE computer society conference on computer vision and pattern recognition*, pages 3485–3492. IEEE, 2010.
- [41] Hantao Yao, Rui Zhang, and Changsheng Xu. Visual-language prompt tuning with knowledge-guided context optimization. *arXiv preprint arXiv:2303.13283*, 2023.
- [42] Renrui Zhang, Ziyu Guo, Wei Zhang, Kunchang Li, Xupeng Miao, Bin Cui, Yu Qiao, Peng Gao, and Hongsheng Li. Pointclip: Point cloud understanding by clip. In *Proceedings of the IEEE/CVF Conference on Computer Vision and Pattern Recognition*, pages 8552–8562, 2022.
- [43] Kaiyang Zhou, Jingkang Yang, Chen Change Loy, and Ziwei Liu. Conditional prompt learning for vision-language models. In *Proceedings of the IEEE/CVF Conference on Computer Vision and Pattern Recognition*, pages 16816–16825, 2022.
- [44] Kaiyang Zhou, Jingkang Yang, Chen Change Loy, and Ziwei Liu. Learning to prompt for vision-language models. *International Journal of Computer Vision*, 130(9):2337–2348, 2022.